



Article

Study on Multiple Effects of Self-Healing Properties and Thermal Characteristics of Asphalt Pavement

Fan Zhang ¹, Yuxuan Sun ¹, Lingyun Kong ^{2,*}, Augusto Cannone Falchetto ^{1,*}, Dongdong Yuan ³ and Weina Wang ²

¹ Department of Civil Engineering, Aalto University, Rakentajanaukio 4, 02150 Espoo, Finland; fan.3.zhang@aalto.fi (F.Z.); yuxuan.sun@aalto.fi (Y.S.)

² National & Local Joint Engineering Research Center of Transportation Civil Engineering Materials, Chongqing Jiaotong University, Chongqing 400074, China; 990201400033@cqjtu.edu.cn

³ School of Highway, Chang'an University, South 2nd Ring Road Middle Section, Xi'an 710064, China; ddy@chd.edu.cn

* Correspondence: konglingyun@cqjtu.edu.cn (L.K.); augusto.cannonefalchetto@aalto.fi (A.C.F.)

Abstract: Asphalt pavements are prone to cracking in low-temperature environments, and microwave heating (MH) can heal the cracks effectively. This research mainly investigates the different MH effects on the self-healing properties of asphalt mixtures. With this objective, the three-point splitting test is conducted to generate the cracks. A microwave oven is employed to heat the samples, and a thermal camera measures the surface temperature. Results indicate that heating power and time show a positive linear correlation with healing efficiency, and the *HI* of the samples can reach over 80%. The *HI* of the samples decreases with the heating cycle, but the sample with reasonable power and time still has a *HI* higher than 70% after 5 cycles. The temperature peaks on thermal images indicate that uneven heating exists during heating, but the heating uniformity is within an acceptable range. The healing efficiency level (*HEL*) suggests that asphalt mixtures have very low inefficient healing behavior if the heating time is below 45 s, but *HEL* can reach 86.14% at 700 W after 60 s. Furthermore, although the *HI* of strength shows ideal results, the recovery of other crack parameters, including stiffness, fracture energy, flexible index, and crack resistance index, are not satisfactory.

Keywords: asphalt mixture; heating time; heating power; heating cycle; crack parameters



Citation: Zhang, F.; Sun, Y.; Kong, L.; Cannone Falchetto, A.; Yuan, D.; Wang, W. Study on Multiple Effects of Self-Healing Properties and Thermal Characteristics of Asphalt Pavement. *Buildings* **2024**, *14*, 1313. <https://doi.org/10.3390/buildings14051313>

Academic Editor: Bjorn Birgisson

Received: 5 April 2024

Revised: 2 May 2024

Accepted: 6 May 2024

Published: 7 May 2024



Copyright: © 2024 by the authors. Licensee MDPI, Basel, Switzerland. This article is an open access article distributed under the terms and conditions of the Creative Commons Attribution (CC BY) license (<https://creativecommons.org/licenses/by/4.0/>).

1. Introduction

Asphalt pavements have become the primary type of road due to their driving comfort, low noise, and short construction period [1–3]. However, the characteristics of asphalt binder confer on the asphalt mixture a viscoelasticity behavior under specific loading conditions with a temperature-dependent response [4,5]. This makes asphalt pavement exhibit different distresses at different temperatures. For example, asphalt mixtures turn soft and show more viscous properties in high-temperature environments [6,7], making them prone to deformation and distress [8–10]. In addition to this, the low-temperature distress of asphalt pavement is particularly noticeable, especially in the Nordic regions. Asphalt binders tend to become brittle when the temperature is lower, causing the pavement to be susceptible to cracking [11,12]. The temperature stress can be generated in low-temperature environments, resulting in the formation of microcracks [13–15]. If the microcracks can not be repaired in time, they can develop into larger cracks or even lead to structural cracks [16]. This can significantly reduce the service life of asphalt pavements and increase maintenance costs. As a result, research in low-temperature regions, such as Finland, has focused more on pavement cracking and repairing [17,18].

Conventional crack maintenance methods typically consist of pouring hot mix asphalt mixtures into cracks and compacting them again [19]. This method requires asphalt mixtures to be pre-mixed. In addition, each of the cracks needs to be grouted. This

method could be more effective and requires significant labor to repair the cracks. In recent studies, the self-healing properties of asphalt pavements have been investigated to promote the repair of cracks [20,21]. The asphalt binder turns to a fluid-like state as temperature increases; it can self-flow into cracks, seal, and partially or fully repair them when the temperature turns back to service temperature [22–24]. Therefore, the self-healing properties of asphalt pavements can be empowered if the binder can rapidly reach an adequate temperature, allowing material mobility. Microwave heating (MH) represents a valuable option for increasing the temperature of asphalt pavement due to the advantages of rapid heating efficiency compared to other heating methods, such as inductive heating [25,26].

In recent years, microwave heating has been applied in pavement maintenance, such as microwave deicing, snow-melting, and healing [17,27–30]. The road can be directly heated based on microwave heating pavement maintenance vehicles, as reported in these papers [17,29]. Gulisano and Gallego summarized the application status of MH technology in asphalt pavement, indicating that the heating process mainly comes from aggregates [31]. Zhang et al. investigated the link between the thermal conductivity, fatigue, and deformation properties of asphalt binders and the MH self-healing of mixtures [32]. Garcia et al. recommended that the optimum moment to heat asphalt mixtures occurs when fatigue life reduces by 35% [33]. In addition, many researchers tried to accelerate the self-healing properties by adding wave-absorbing materials, such as carbon nanotubes, steel slag, and steel fibers, to asphalt binders or mixtures [21,32,34,35]. The asphalt mixtures can also be prefabricated as the self-healing tack coat to extend the pavement life, which was reported in these papers [36,37].

According to the above literature review, MH has been successfully applied in asphalt pavement rehabilitation. However, there are still a number of limitations on the self-healing properties of asphalt mixtures by MH. First, MH is a complex multifactorial process, with different heating times, powers, frequencies, and cycles affecting the self-healing results of asphalt mixtures. Second, the fracture process of asphalt mixtures is similarly complex, and previous research has focused almost exclusively on strength recovery, with fewer studies on other fracture parameters [13,20,27,32].

Consequently, the objective of this study is to explore the multiple effects of MH on self-healing properties, with the evaluation of these properties being conducted across various crack parameters. For this purpose, semi-circular samples are prepared to carry out three-point bending (3PB) tests to generate cracks in the specimens. The cracked samples are then healed by a microwave oven at different times, powers, and cycles to investigate the multiple effects on self-healing properties. An infrared camera is utilized to measure the surface temperature of the asphalt mixtures with different MH factors during radiation. Finally, the crack parameters of the samples are also compared before and after healing. The testing results are evaluated and analyzed in three aspects: (1) the healing effect of heating time, power, and cycle; (2) thermal transfer characteristics during microwave radiation; and (3) crack parameter analysis before and after healing. Furthermore, conclusions can be drawn based on the result analysis.

2. Materials and Methods

2.1. Materials

The basic materials include asphalt binders, aggregate, and fillers. The asphalt binders used in this research are 60/80 neat binders; their physical properties meet all the requirements according to JTG E20 2011 [38]. The aggregate and fillers are natural limestones, and their basic properties also meet the requirement of JTE E42 2005 [39].

2.2. Sample Preparation

All the basic materials are mixed together to prepare the Marshall samples. The asphalt binder content is 4.9%, determined by JTG E20 2011 [38], and the filler content is 5%. An AC-13 (asphalt concrete with an NMA (nominal maximum aggregate size) of 13 mm)

type of asphalt mixture sample with an air void between 3% and 5% is selected [38]; its gradation curve is displayed in Figure 1. Then, a typical Marshall sample with a 101.6 mm in diameter and a 63.5 mm in height is cut into semi-circular specimens. Each side of the Marshall specimen is cut by about 6.5 mm to avoid the effect of uneven density on the experimental results [40]. The remaining specimen is then cut in the center, and two cylindrical specimens with the same diameter and a height of about 25 mm are obtained. Next, each of the cylindrical specimens is cut in half to obtain two semi-circular specimens. Finally, a 3 mm \times 10 mm notch seam is prepared at the bottom center of each semi-circular specimen to facilitate the formation of cracks; the preparation process is presented in Figure 2. Generally, the specimen for the semi-circular bending test is prepared from rotary compaction specimens with a diameter of 150 mm. However, due to the convenience of the Marshall specimen preparation and the fact that smaller sizes are more convenient to place in a microwave oven to measure the temperature, the smaller Marshall specimen is chosen for preparing the semi-circular specimens in this study.

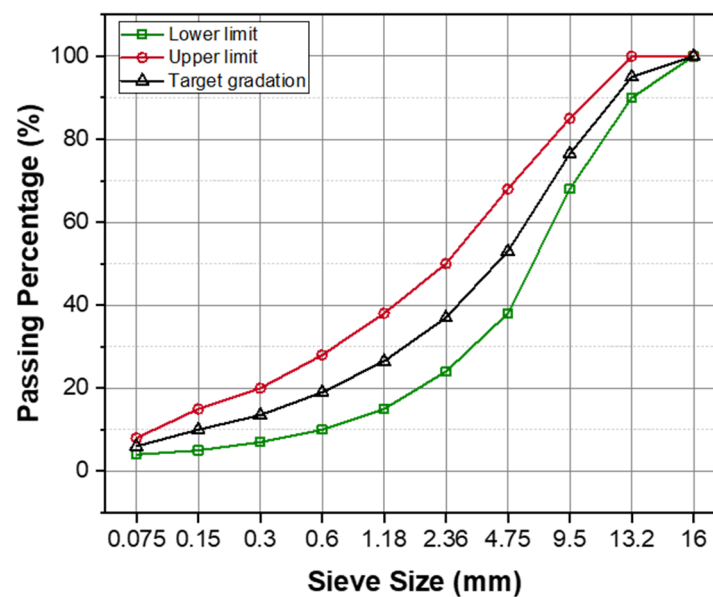


Figure 1. Gradation curve of AC-13.

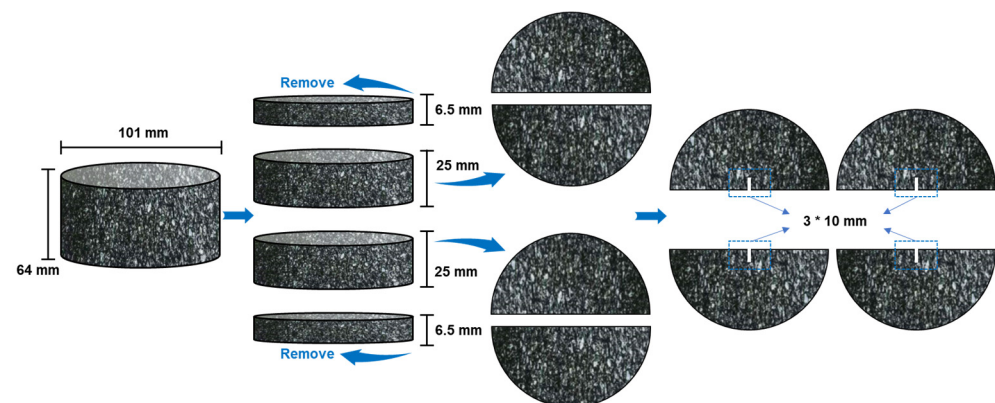


Figure 2. Sample preparation process.

2.3. Three-Point Bending Test

This test can evaluate the low-temperature crack performance of asphalt mixtures, which is conducted via a MTS machine. Before the test, all the specimens are placed at room temperature for 48 h to exclude the moisture effect. The semi-circular specimens are first conditioned in a thermostatic chamber at $-20\text{ }^{\circ}\text{C}$ for 2 h and then placed on the testing

frame, which is shown in Figure 3. A vertical load with a rate of 0.5 mm/min is applied to induce the formation and propagation of a crack. The test is finished when the applied load is lower than half of the peak load. The peak load, stress, and strain can be obtained from the test data, and these parameters can be used for calculating fracture energy (G_f), fracture toughness (K_{IC}), and crack resistance index (CRI) before and after healing according to JTG E20 2011 [38]. The stiffness can be determined from the slope of the initial phase of the stress–strain curve.

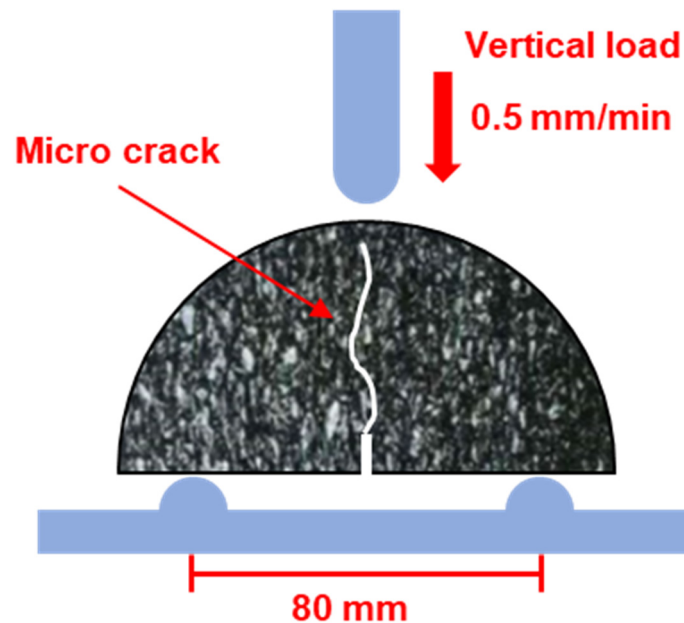


Figure 3. Sample placement of SCB test.

It should be noted that this test has some differences with the conventional semi-circular bending (SCB) test. First, the termination condition is when the load is reduced to half of the peak load. This can ensure that the samples are not completely destroyed and can not be repaired, but at the same time, microcracks can be generated. Secondly, the diameter of the samples is 100 mm, not the conventional 150 mm. This size is more suitable for the normal microwave oven for the easy heating of the samples. The application of this method was also used in other studies [32,41,42].

2.4. Microwave Healing Test

The damaged SCB specimens can recover their properties to a certain extent after microwave heating due to the self-healing behavior of the mixture associated with the mobility of the asphalt binders. The damaged SCB specimens are first placed at room temperature to dry the water on the surface caused by low-temperature conditioning. Then, a microwave oven with 700 W of outpower and 2.45 GHz frequency is used to perform the heating procedure. The heating time is 60 s to avoid the excessive softening of the mixtures. After heating, the specimens are put in a thermostatic box at room temperature for 12 h to facilitate the repair of the cracks. This process consists of one cycle of the damage-healing process, and a total of 5 cycles are performed in this study. The healing index can be defined by the peak load ratio before and after healing based on the literature review, as shown in Equation (1) [13,32]. An infrared camera is utilized to measure the temperature of the specimens every 15 s during heating, as shown in Figure 4. The thermal images obtained from the infrared camera can then be transferred to the temperature data to quantitatively analyze the thermal characteristics of the asphalt mixtures. Based on previous research, asphalt mixture can achieve excellent self-healing properties when the surface temperature reaches 90 °C [32,35]. In addition, the mixtures start showing self-healing behavior when the temperature is above the softening point of the binder. Hence, the temperature between

this range can be considered the effective healing temperature, and the healing efficiency level can be defined in Equation (2).

$$HI_i = \frac{P_i}{P_0} \times 100\% \quad (1)$$

where HI_i (%) is the healing index of the i th time; P_i (kN) and P_0 (kN) are the peak loads of the i and initial time.

$$HEL = \frac{A_{effective}}{A_{total}} \times 100\% \quad (2)$$

where HEL (%) is the healing efficiency level; $A_{effective}$ is the surface area where the temperature is in the effective healing temperature range; A_{total} is the entire area of the specimen.

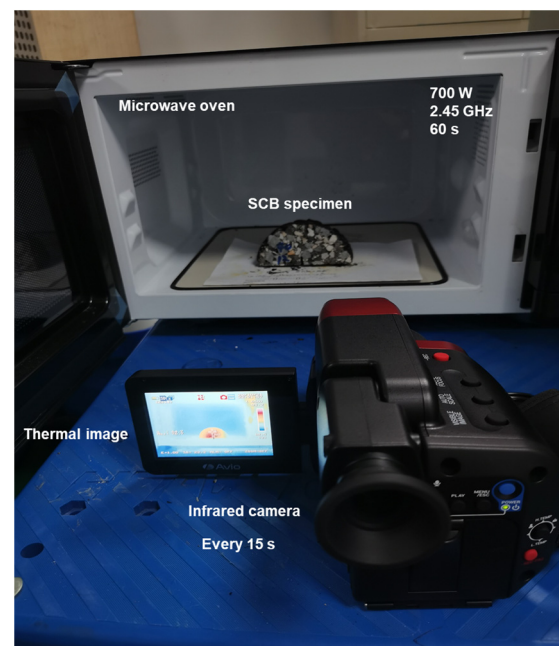


Figure 4. Microwave heating and temperature measurement process.

3. Results and Discussion

3.1. Healing Effect of Asphalt Mixtures

The healing properties can be evaluated based on HI , defined in Section 2.4. The healing efficiency can be affected by multiple factors, such as heating time, heating output power, and heating cycle. Figure 5 shows the healing efficiency of the asphalt mixtures with different heating times. It can be found that the HI is much higher when the heating time is longer at 120 W. The HI s of asphalt mixtures with 15 s and 30 s of heating times are both lower than 30%; this healing level can not be considered effective based on previous research [32]. The asphalt mixture has the potential to crack again. However, the HI increases to above 60% when the heating time is longer than 45 s. When the output power is 280 W, the samples with longer heating time also possess better healing properties. The HI of the asphalt mixtures with 60 s heating time is 70.92%, which is 1.466, 1.474, and 1.25 times that of the samples with 15 s, 30 s, and 45 s heating time, respectively. When the output power is 540 W, all the samples' HI s are higher than 50%; this means the strength of the mixtures can be recovered by half of the initial value. When the output power is 700 W, the healing efficiency has a strong linear relationship with the heating time. It can be found that the HI of asphalt mixtures with 15 s heating time is 55.59%, and the HI can increase by 17.72%, 26.34%, and 47.91%, respectively. The lack of a significant linear relationship between heating time and HI at the first three output powers can be attributed to the different heating modes of the microwave oven. The microwave oven can continue to heat

when the output power is 700 W. However, the microwave oven can heat up intermittently when the output power is lower than 700 W, this is reported in Lou's research [42]. Hence, a long, continuous heating time leads to better healing efficiency. This can also be verified in Figure 5, where the samples after 60 s of microwave radiation always have higher *HI* values than the samples at other radiation times at all different output powers.

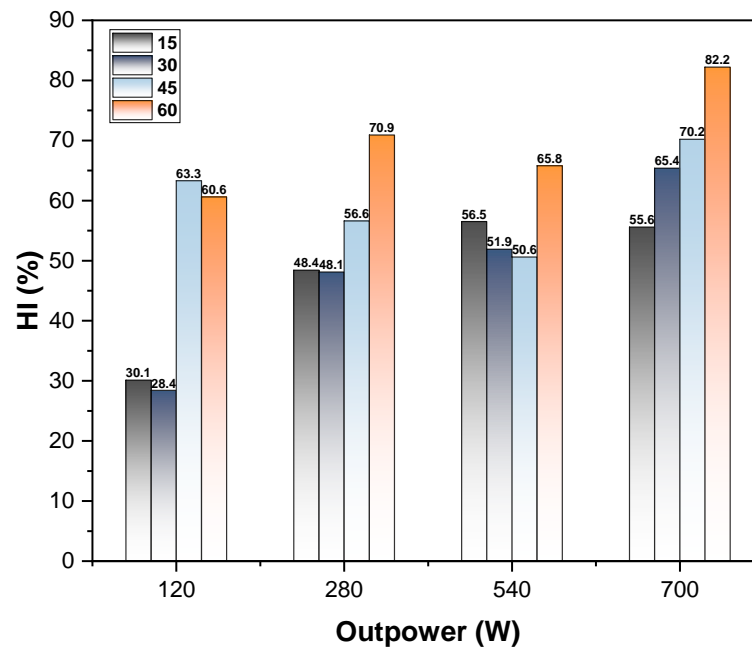


Figure 5. *HI* of samples with different heating times.

The *HI* of the samples with different output powers is shown in Figure 6. It can be found that the *HI* basically increases with the output power. When the heating time is 15 s, the samples with 120 W output power have the lowest *HI* of 30.05%. *HI* can then increase to 48.37%, 56.47%, and 55.59% with 280 W, 540 W, and 700 W output powers, respectively. The samples with 120 W output power still show the lowest healing efficiency after 30 s, which is 28.43%. The *HI*s of the other samples are obviously higher than in the latter case; their *HI*s can increase by 69.17%, 82.51%, and 130.22% with 280 W, 540 W, and 700 W output powers. This reveals that the healing efficiency is too low to apply microwave heating technology when the heating power and time are both small. This finding is consistent with the conclusions of Zhu's work in 2020 [43]. When the heating time is above 30 s, the healing efficiency increases. The samples with different output powers after 45 s of radiation time show similar *HI* values. Their *HI*s are all between 50.6% and 70.23%. When the heating time is 60 s, the samples with 700 W of output power have the highest *HI* of 82.23%, which is 1.26, 1.16, and 1.25 times that of the samples with 120 W, 280 W, and 540 W. From Figure 6, it can be revealed that the higher the output power, the better the healing efficiency is. The samples obviously can not meet the high-efficiency healing requirement when the heating power is small (120 W) and the heating time is low (below 30 s).

Figure 7 shows the *HI* values of the samples with different heating powers and cycles after 60 s radiation time. All the curves have downward trends with the heating cycles, which suggests that the healing properties have become worse. Frequent heating can have an aging effect on the asphalt mixtures according to the previous research basis, reducing the viscous properties of the asphalt binders [44,45]. Besides, the softening point of the aged binder is higher, which increases the initial healing temperature of the samples [44]. As a result, the *HI* of the samples decreases with the increase in the heating cycle. It can be clearly observed that the samples with 700 W power always have the highest *HI* during five cycles; they are 82.23%, 80.98%, 75.47%, 78.64%, and 74.75%, respectively. Obviously, the samples with 120 W power have the lowest *HI* during five cycles, which are 60.62%,

35.54%, 34.38, 27.62%, and 19.34%, respectively. When reaching the last heating cycle (cycle five), the samples with 700 W can still possess a *HI* higher than 80%. This *HI* is 1.52, 2.20, and 3.87 times that of the samples with 540 W, 280 W, and 120 W powers. Similarly, the *HI* of the samples with 700 W of power and 60 s of time is higher than that of the same samples with the same heating conditions, as reported in Zhu's work [43]. Hence, it can be concluded that 700 W of the output power is the optimum heating power among those adopted in this research.

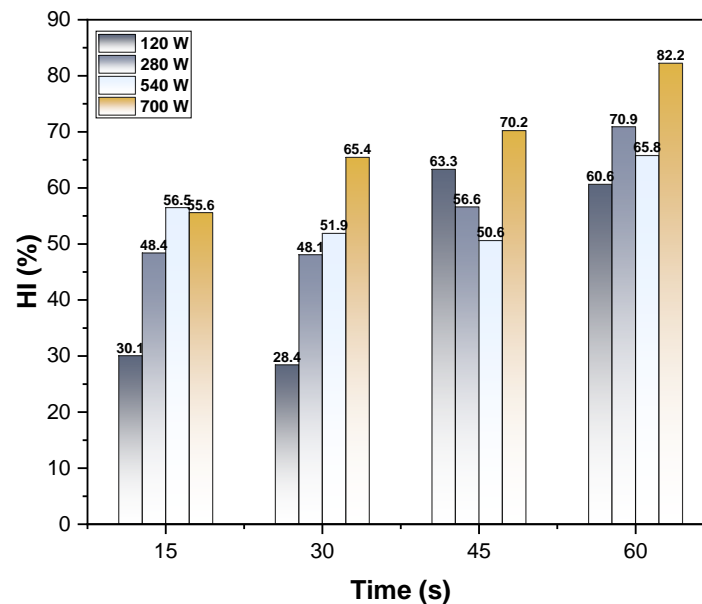


Figure 6. *HI* of samples with different output powers.

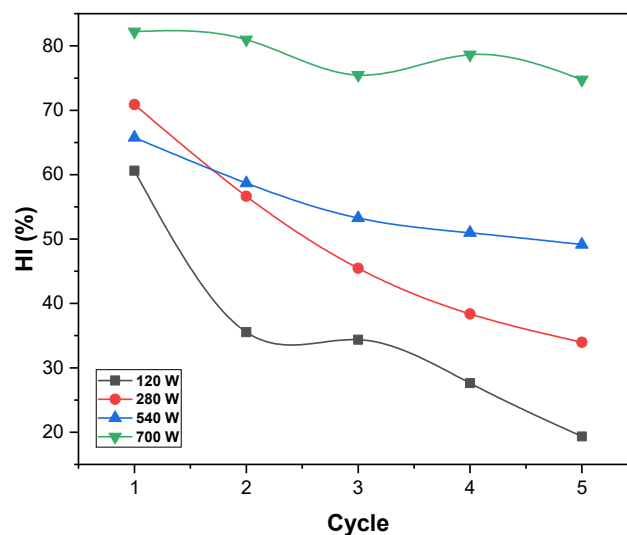


Figure 7. *HI* of samples with different cycles.

3.2. Thermal Transfer Characteristic

The self-healing mechanism is a consequence of the increased mobility of asphalt binders at higher temperatures, allowing the material to flow into cracks and repair them during microwave radiation [22–24]. Such a process requires that the temperatures of the samples be higher than the softening point of the binders. The thermal images in Figure 8 demonstrate the thermal characteristics of the samples during microwave heating. The surface temperatures of all the samples are basically the same without much difference after 15 s. Then, temperatures are concentrated at one or multiple points on the samples.

This part of the concentrated heat gradually spreads to the entire volume of the specimen, thus increasing the temperature of the surrounding environment. Therefore, from Figure 8, it can be observed that temperature peaks increase gradually in intensity, and the diffusion area turns bigger with heating time. The reason for this uneven heating is due to the different wave-absorbing properties of the materials in the mixtures, with better absorbing properties of aggregate compared to binders [17,46]. Asphalt binder is a low wave-sensitive material, while aggregates are sensitive, causing the inconsistent increase in temperature. Besides, although there are no other additives in the mixtures, different sizes of the same aggregate can have various microwave-heating properties, for example, Gao et al. indicated that 4.75–9.5 mm of aggregate shows excellent wave-absorbing properties [47]. Hence, it is necessary to investigate the heating temperature and differences to control uneven heating.

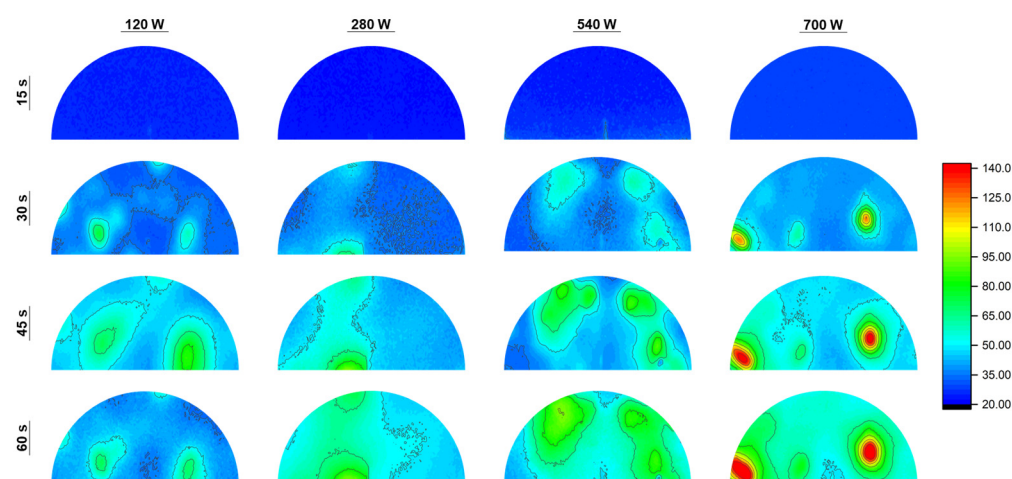


Figure 8. Thermal images of the samples with different powers and times.

Figure 9 shows the surface temperature of the asphalt mixtures with different powers during microwave radiation. The temperatures of all the samples are close to 25 °C when the heating time is 15 s. This condition indicates that the asphalt mixtures do not absorb enough microwave energy to be converted into heat energy. Then, the temperatures of the samples increase with heating time. The surface temperatures of the samples with 120 W, 280 W, 540 W, and 700 W powers can achieve 2.00, 2.42, 2.42, and 2.24 times their initial temperatures after 60 s. In terms of heating power, the surface temperature also rises linearly with the heating power, but it is not obvious within a short heating time (within 30 s). Temperature and power show a stepwise linear relationship when heating time is 45 s and 60 s. The temperature-rising mechanism is the same as the previous work, and they all show a linear relation with heating power and time, but there exist some differences in detailed data [43].

A higher temperature makes it easier to melt the asphalt binders and heal cracks, but the healing properties are also affected by the uniformity of the temperature distribution. If the heating is not uniform, one part of the mixture may be too hot and cause the aging of the binders; the temperature of the other part may be too low to heal the cracks [44,45,48]. This uneven heating can not be avoided because the mix is a heterogeneous material, so the heating uniformity needs to be controlled within a reasonable range. Figure 10 shows the standard deviation (St.d) of the samples after heating; this parameter allows for a quantitative evaluation of the heating uniformity. The lower energy absorbed by the mix makes the temperature difference smaller, resulting in a lower St.d at 15 s. Similarly, St.d increases with the heating time, suggesting the temperature differences turn larger with a longer heating time. The highest St.d of the samples with 120 W, 280 W, 540 W, and 700 W is 8.96 °C, 9.64 °C, 13.06 °C, and 19.5 °C occurring at 60 s. These values are considered within a reasonable range based on the previous research [13,32,47]. In addition, the heating uniformity deteriorates with heating time and power. It can be explained by the fact that

the wave-sensitive material in the mixture warms up more quickly when heating power and time are both higher.

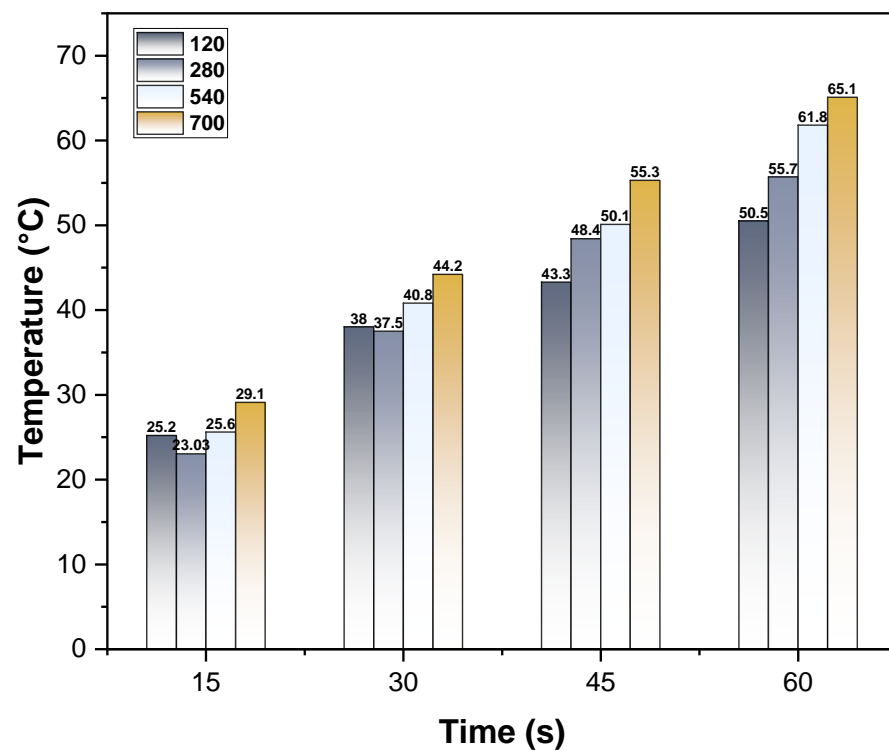


Figure 9. Surface temperature of the samples with different powers and times.

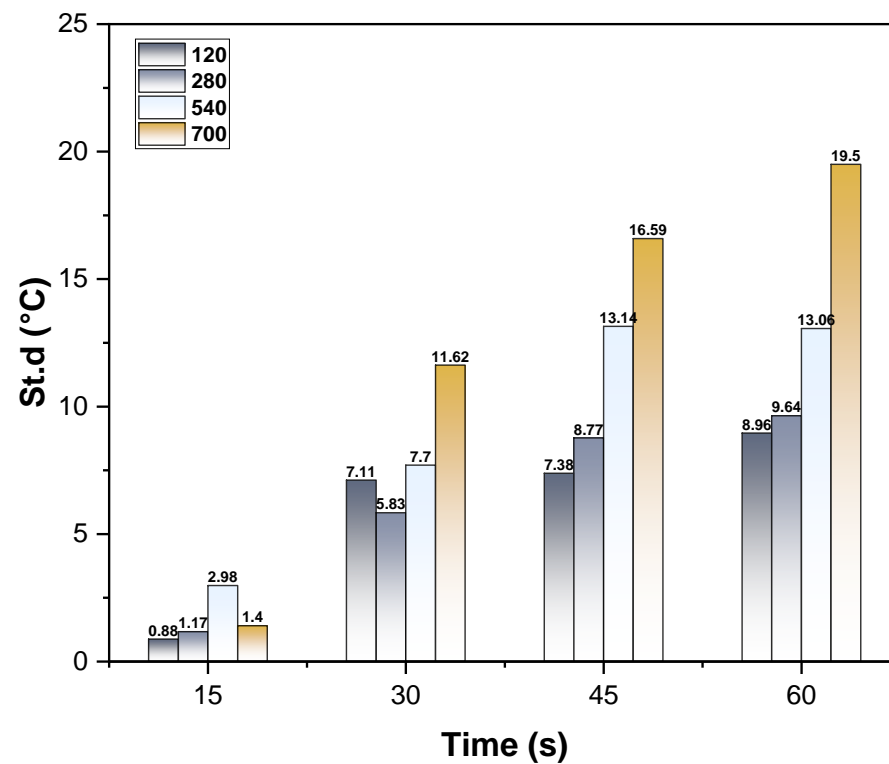


Figure 10. St.d of the samples with different powers and times.

A high-temperature environment can promote the self-healing properties of the asphalt mixtures, but excessive temperatures can also cause overheating issues and damage to

binders. *HEL* can evaluate the effective healing area of the mixture based on the definition in Section 2.4, and its result is shown in Figure 11. It can be observed that the *HEL* of all the samples is 0% after 15 s of microwave heating. This indicates that the temperature of asphalt binders is still below their softening point and keeps a solid state. The asphalt binders can not flow into the cracks and do not possess self-healing behavior. After 30 s of radiation, all the samples start to heal the cracks with a very low efficiency (below 20%). From 45 s, the *HEL* of samples with 120 W power is much lower than that of other samples. In addition, the *HEL* also begins to be linearly distributed with the heating power. The *HEL* of the samples with 120 W, 280 W, 540 W, and 700 W is 41.7%, 64.42%, 80.5%, and 86.14%. A higher power and time can achieve the highest *HEL* value. It should be noted that all the *HEL*s increase with radiation time, but *HEL* will decrease when more temperatures exceed the effective healing range than enter the range. This conclusion has been identified by these papers [13,32]. The *HEL* curves in Figure 11 do not show a downward trend within 60 s, suggesting that all the samples do not have overheating issues with this heating time. In addition, the samples with 700 W of power can achieve the highest *HI* (82.23%) and *HEL* (86.14%) after 60 s of heating time. Hence, it is recommended that the AC-13 samples be microwave-heated at 700 W for 60 s.

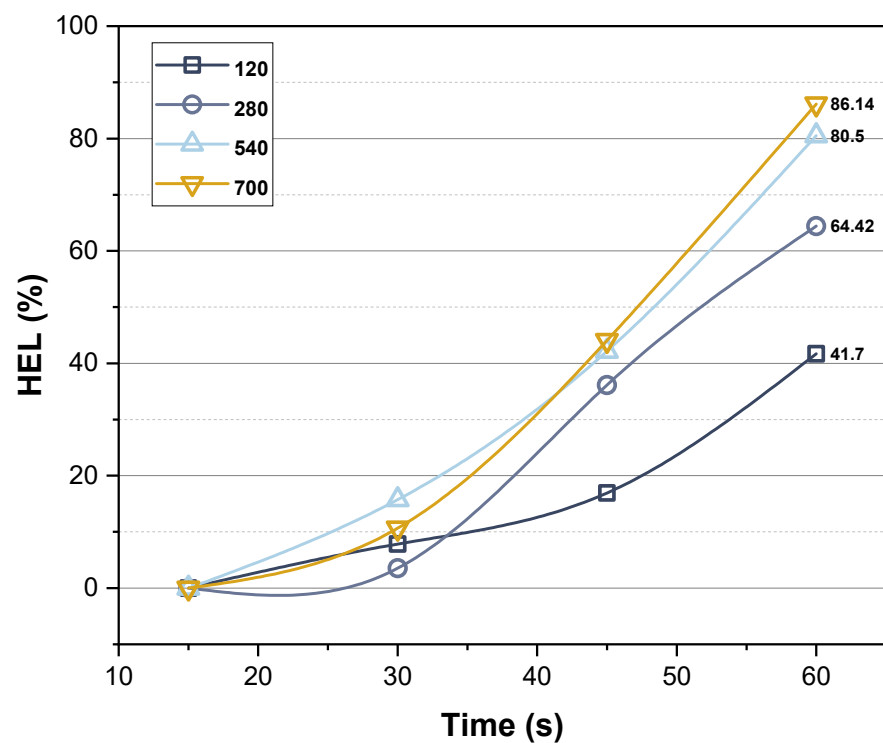


Figure 11. *HEL* of the samples with different powers and times.

3.3. Crack Parameters of Asphalt Mixtures

The healing index in the previous research has mainly been defined by the strength ratio of the mix before and after healing [13,32]. However, the fracture recovery of the mixes should be evaluated in terms of different properties, and a single evaluation of strength is limited. The highest *HI* of strength is noticeable in the samples with 700 W of power and 60 s of heating time after one cycle. Hence, the *HI* of this sample is further investigated in this section in terms of fracture energy (G_f), fracture toughness (K_{IC}), crack resistance index (*CRI*), and stiffness. These parameters can be defined by Equations (3)–(5) and Figure 12.

$$G_f = \frac{W_f}{A_{ing}} \times 10^6 \quad (3)$$

$$FI = \frac{G_f}{|m|} \times A \quad (4)$$

$$CRI = \frac{G_f}{P_{max}} \quad (5)$$

where G_f is the fracture energy (J/m^2); W_f is fracture work (J), which can be obtained from Figure 12; A_{ing} is ligament area (mm^2); FI is the flexible index; m is the absolute value of the slope of the tangent line, which can be obtained in Figure 12; $A = 0.01$; CRI is the crack resistance index (J/kN); P_{max} is peak load in Figure 12.

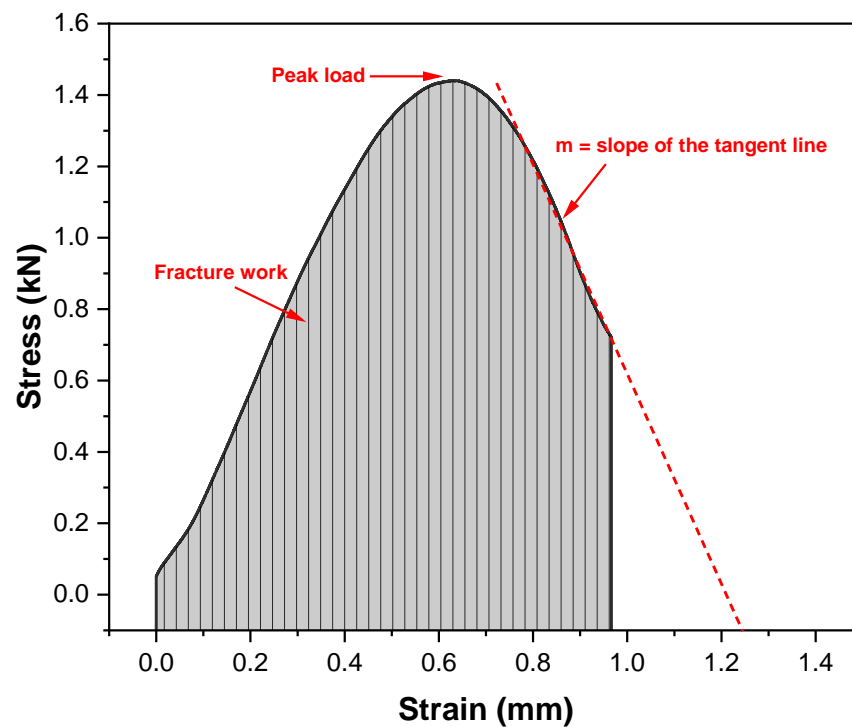


Figure 12. Stress–strain curve of the 3PB test.

Figure 13 represents these crack parameters of the samples before and after healing. The stiffness of the samples after healing is higher than that before healing. This means that a smaller strain is required if the sample cracks again [49]. This is because microwave healing only partially restores the mixture's properties, making it more susceptible to secondary cracking. The G_f of the samples before and after healing is $846.08 \text{ J}/\text{m}^2$ and $310.01 \text{ J}/\text{m}^2$, which only restore 36.04% of the initial G_f . Similarly, the FI of the samples also reduces after healing, which is 33.46% of the FI before healing. The CRI of the samples recovers more than the above parameters, at 44.56%. However, this value is still below 50%, and the samples with a CRI of $215.27 \text{ J}/\text{kN}$ after healing are easier to crack again. Although the strength of the samples after healing can be recovered up to 80%, the other crack parameters also need to be considered.

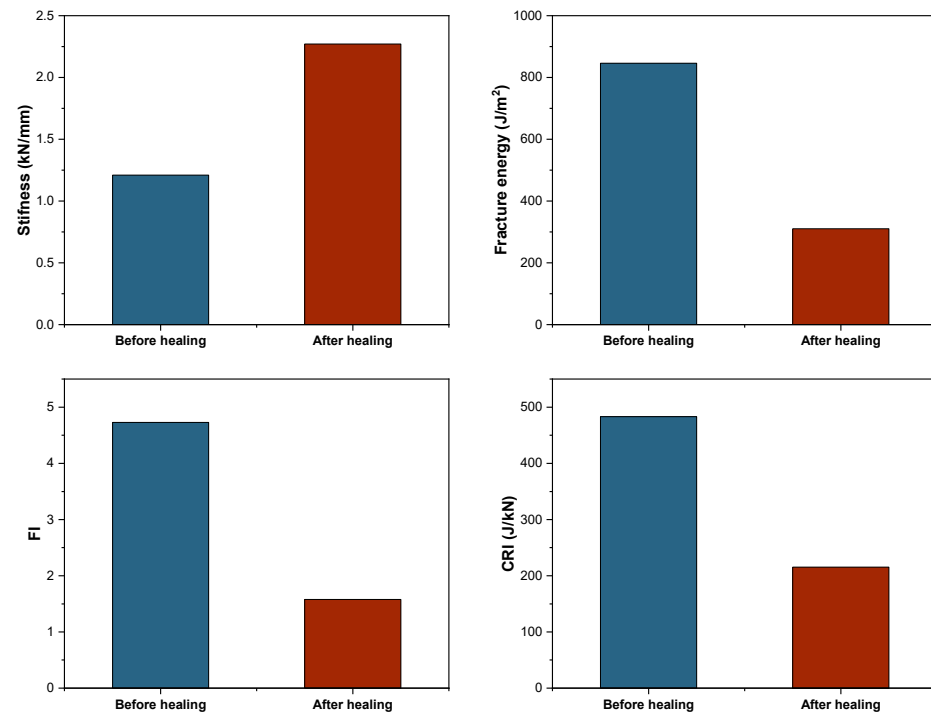


Figure 13. Crack parameters of the samples before and after healing.

4. Conclusions

This study investigates the various effects of microwave heating on the self-healing properties of asphalt mixtures, including heating time, power, and cycle, based on three three-point bending tests and microwave heating technology. In addition, the surface temperatures are recorded during microwave radiation to investigate the thermal transfer characteristics of samples, and the crack parameters are also compared before and after healing. The main conclusions can be drawn as follows:

- (1) Heating time and power that are too low are not enough to heal the asphalt mixture; on the contrary, 60 s heating time at 700 W power can restore the strength of the asphalt mixture to more than 80%.
- (2) There is a linear correlation between the healing level of the asphalt mixture and the heating time and power, and this relationship continues to exist as the heating cycle increases.
- (3) Asphalt mixture temperature uniformity can be observed in the heating process, and the temperature turns more uneven with the heating time and power increase.
- (4) The asphalt mixture does not have a healing behavior at the beginning of microwave radiation, but the effective healing area increases with time up to more than 80%.
- (5) Microwave heating can promote the recovery of the strength of asphalt mixtures. However, other crack parameters, including fracture energy, flexible index, and crack resistance index, all recovered at less than 50%.

Based on the conclusions, MH can be considered to be a promising pavement maintenance method. Some waste slags, such as steel slag, have excellent wave-absorbing properties, and using slags as road aggregates have been identified. Hence, replacing conventional aggregate with slags has the potential to accelerate self-healing properties, and this also can provide a solution for waste disposal, which will be further investigated in the future work.

Author Contributions: Conceptualization, F.Z.; methodology, F.Z.; validation, F.Z.; formal analysis, F.Z. and Y.S.; investigation, F.Z.; data curation, F.Z.; writing—original draft preparation, F.Z. and A.C.F.; writing—review and editing, F.Z. and A.C.F.; visualization, F.Z. and D.Y.; supervision, A.C.F.;

project administration, F.Z., L.K. and W.W.; funding acquisition, F.Z., L.K. and W.W. All authors have read and agreed to the published version of the manuscript.

Funding: This research was funded by “The National & Local Joint Engineering Research Center of Transportation and Civil Engineering Materials, Chongqing Jiaotong University, grant number: TCEM-2023-02” and “The National Natural Science Foundation of China, grant number: 52078091”.

Data Availability Statement: The original contributions presented in the study are included in the article, further inquiries can be directed to the corresponding author.

Conflicts of Interest: The authors declare no conflicts of interest.

References

1. Zhao, Q.; Li, Z.; Hu, W.; Meng, X.; Zhang, H. Driving comfort evaluation for manhole covers and pavement around manholes. *Adv. Mater. Sci. Eng.* **2019**, *2019*, 1293619. [\[CrossRef\]](#)
2. Al-Qadi, I.L.; Elseifi, M.A. New generation of wide-base tires: Impact on trucking operations, environment, and pavements. *Transp. Res. Rec.* **2007**, *2008*, 100–109. [\[CrossRef\]](#)
3. Li, H.; Nyirandayisabye, R.; Dong, Q.; Niyirora, R.; Hakuzweyezu, T.; Zardari, I.A.; Nkinahamira, F. Crack damage prediction of asphalt pavement based on tire noise: A comparison of machine learning algorithms. *Constr. Build. Mater.* **2024**, *414*, 134867. [\[CrossRef\]](#)
4. Huang, T.; Wang, Z.; Dong, H.; Qin, H.; Liu, H.; Cao, Z. Time-Temperature-Stress Equivalent Characteristics and Nonlinear Viscoelastic Model of Asphalt Mixture under Triaxial Compressive Stress State. *J. Mater. Civ. Eng.* **2024**, *36*, 04023543. [\[CrossRef\]](#)
5. Jahanbakhsh, H.; Karimi, M.M.; Nejad, F.M.; Jahangiri, B. Viscoelastic-based approach to evaluate low temperature performance of asphalt binders. *Constr. Build. Mater.* **2016**, *128*, 384–398. [\[CrossRef\]](#)
6. Zhang, F.; Hu, C. Preparation and properties of high viscosity modified asphalt. *Polym. Compos.* **2017**, *38*, 936–946. [\[CrossRef\]](#)
7. Atul Narayan, S.P.; Murali Krishnan, J.; Little, D.N.; Rajagopal, K.R. Mechanical behaviour of asphalt binders at high temperatures and specification for rutting. *Int. J. Pavement Eng.* **2017**, *18*, 916–927. [\[CrossRef\]](#)
8. Pokorski, P.; Radziszewski, P.; Sarnowski, M. Study of high-temperature properties of asphalt mixtures used for bridge pavement with concrete deck. *Materials* **2021**, *14*, 4238. [\[CrossRef\]](#) [\[PubMed\]](#)
9. Abouelsaad, A.; White, G. Review of asphalt mixture ravelling mechanisms, causes and testing. *Int. J. Pavement Res. Technol.* **2021**, *15*, 1448–1462. [\[CrossRef\]](#)
10. Li, J.; Guo, W.; Meng, A.; Han, M.; Tan, Y. Investigation on the micro deformation mechanism of asphalt mixtures under high temperatures based on a self-developed laboratory test. *Materials* **2020**, *13*, 1791. [\[CrossRef\]](#)
11. Office, J.E.; Cavalli, M.C.; Chen, D.; Chen, Q.; Chen, Y.; Falchetto, A.C.; Fang, M.; Gu, H.; Han, Z.; He, Z.; et al. Review of advanced road materials, structures, equipment, and detection technologies. *J. Road Eng.* **2023**, *3*, 370–468.
12. Ishaq, M.A.; Giustozzi, F. Correlation between rheological tests on bitumen and asphalt low temperature cracking tests. *Constr. Build. Mater.* **2022**, *320*, 126109. [\[CrossRef\]](#)
13. Zhang, F.; Sha, A.; Cao, Y.; Wang, W.; Song, R. Microwave heating moment, thermal characteristics, and structural variations of different steel slag asphalt mixtures suffered from freeze-thaw damage. *Cold Reg. Sci. Technol.* **2024**, *217*, 104028. [\[CrossRef\]](#)
14. Al-Qudsi, A.; Falchetto, A.C.; Wang, D.; Büchler, S.; Kim, Y.S.; Wistuba, M.P. Finite element cohesive fracture modeling of asphalt mixture based on the semi-circular bending (SCB) test and self-affine fractal cracks at low temperatures. *Cold Reg. Sci. Technol.* **2020**, *169*, 102916. [\[CrossRef\]](#)
15. Khawaja, H.; Tanveer, A. Review of low-temperature crack (LTC) developments in asphalt pavements. *Int. J. Multiphysics* **2018**, *12*, 169–187.
16. Tang, J.; Fu, Y.; Ma, T.; Zheng, B.; Zhang, Y.; Huang, X. Investigation on low-temperature cracking characteristics of asphalt mixtures: A virtual thermal stress restrained specimen test approach. *Constr. Build. Mater.* **2022**, *347*, 128541. [\[CrossRef\]](#)
17. Zhang, F.; Wang, D.; Falchetto, A.C.; Cao, Y. Microwave deicing properties and carbon emissions assessment of asphalt mixtures containing steel slag towards resource conservation and waste reuse. *Sci. Total Environ.* **2024**, *912*, 169189. [\[CrossRef\]](#) [\[PubMed\]](#)
18. Roimela, P.; Salmenkaita, S.; Maijala, P.; Saarenketo, T. Road analysis: A tool for cost-effective rehabilitation measures for Finnish roads. In Proceedings of the Eighth International Conference on Ground Penetrating Radar, Gold Coast, Australia, 27 April 2000; Volume 4084, pp. 107–112.
19. Zhu, Z.; Cai, W.; Liu, W. Research on Disposal Parameters and Diffusion Path of Asphalt Pavement Crack Grouting. *J. Munic. Technol.* **2023**, *41*, 24–29+47.
20. Anupam, B.R.; Sahoo, U.C.; Chandrappa, A.K. A methodological review on self-healing asphalt pavements. *Constr. Build. Mater.* **2022**, *321*, 126395. [\[CrossRef\]](#)
21. Agzenai, Y.; Pozuelo, J.; Sanz, J.; Perez, I.; Baselga, J. Advanced self-healing asphalt composites in the pavement performance field: Mechanisms at the nano level and new repairing methodologies. *Recent Pat. Nanotechnol.* **2015**, *9*, 43–50. [\[CrossRef\]](#)
22. Roja, K.L.; Padmarekha, A.; Krishnan, J.M. Rheological investigations on warm mix asphalt binders at high and intermediate temperature ranges. *J. Mater. Civ. Eng.* **2018**, *30*, 04018038. [\[CrossRef\]](#)

23. Karimi, M.M.; Amani, S.; Jahanbakhsh, H.; Jahangiri, B.; Alavi, A.H. Induced heating-healing of conductive asphalt concrete as a sustainable repairing technique: A review. *Clean. Eng. Technol.* **2021**, *4*, 100188. [\[CrossRef\]](#)
24. Adam, Q.F.; Levenberg, E.; Ingeman-Nielsen, T.; Skar, A. Modeling the use of an electrical heating system to actively protect asphalt pavements against low-temperature cracking. *Cold Reg. Sci. Technol.* **2023**, *205*, 103681. [\[CrossRef\]](#)
25. Liu, C.; Leng, L. Application of Microwave Heating Technology in Pothole Repair. *J. Munic. Technol.* **2023**, *41*, 42–46.
26. Zhang, J.; Gao, L.; Dong, Z. Review on Materials and Technology of Multifunctional Maintenance of Asphalt Pavement. *J. Munic. Technol.* **2023**, *41*, 80–93.
27. Zhang, L.; Zhang, Z.; Yu, W.; Miao, Y. Review of the Application of Microwave Heating Technology in Asphalt Pavement Self-Healing and De-icing. *Polymers* **2023**, *15*, 1696. [\[CrossRef\]](#)
28. Wu, W.; Jiang, W.; Xiao, J.; Yuan, D.; Wang, T.; Ling, X. Investigation of LAS-based fatigue evaluation methods for high-viscosity modified asphalt binders with high-content polymers. *Constr. Build. Mater.* **2024**, *422*, 135810. [\[CrossRef\]](#)
29. Gao, J.; Guo, H.; Wang, X.; Wang, P.; Wei, Y.; Wang, Z.; Huang, Y.; Yang, B. Microwave deicing for asphalt mixture containing steel wool fibers. *J. Clean. Prod.* **2019**, *206*, 1110–1122. [\[CrossRef\]](#)
30. Fakhri, M.; Javadi, S.; Sedghi, R.; Sassani, A.; Arabzadeh, A.; Baveli Bahmai, B. Microwave induction heating of polymer-modified asphalt materials for self-healing and deicing. *Sustainability* **2021**, *13*, 10129. [\[CrossRef\]](#)
31. Gulisano, F.; Gallego, J. Microwave heating of asphalt paving materials: Principles, current status and next steps. *Constr. Build. Mater.* **2021**, *278*, 121993. [\[CrossRef\]](#)
32. Zhang, F.; Sha, A.; Cao, Y.; Wang, W.; Song, R.; Jiao, W. Characterization of Self-healing Properties of Asphalt Pavement Materials Containing Carbon Nanotubes: From the Binder and Mix Level based on Grey Relational Analysis. *Constr. Build. Mater.* **2023**, *404*, 133323. [\[CrossRef\]](#)
33. Garcia, A.; Salih, S.; Gómez-Mejide, B. Optimum moment to heal cracks in asphalt roads by means electromagnetic induction. *Constr. Build. Mater.* **2020**, *238*, 117627. [\[CrossRef\]](#)
34. Lu, D.; Jiang, X.; Leng, Z.; Huo, Y.; Wang, D.; Zhong, J. Electrically conductive asphalt concrete for smart and sustainable pavement construction: A review. *Constr. Build. Mater.* **2023**, *406*, 133433. [\[CrossRef\]](#)
35. Gallego, J.; del Val, M.A.; Contreras, V.; Pérez, A. Heating asphalt mixtures with microwaves to promote self-healing. *Constr. Build. Mater.* **2013**, *42*, 1–4. [\[CrossRef\]](#)
36. Dong, Y.S.; Hou, Y.; Wang, Z.F.; Qian, Z.Y. Self-healing performance of rollable asphalt mixture. *J. Mater. Civ. Eng.* **2019**, *31*, 04019117. [\[CrossRef\]](#)
37. Wang, F.; Zhang, H.; Liu, K.; Liu, H.; Zhang, X. Development of self-heating tack coat for bonding prefabricated rollable asphalt materials to existing pavement structure. *Constr. Build. Mater.* **2023**, *409*, 133937. [\[CrossRef\]](#)
38. *JTG E20-2011*; Standard Test Methods of Bitumen and Bituminous Mixtures for Highway Engineering. People's Communication Press: Beijing, China, 2011.
39. *JTG E42-2005*; Test Methods of Aggregate for Highway Engineering. People's Communication Press: Beijing, China, 2005.
40. Mandal, T.; Ling, C.; Chaturabong, P.; Bahia, H.U. Evaluation of analysis methods of the semi-circular bend (SCB) test results for measuring cracking resistance of asphalt mixtures. *Int. J. Pavement Res. Technol.* **2019**, *12*, 456–463. [\[CrossRef\]](#)
41. Liu, J.; Wang, Z.; Jia, H.; Jing, H.; Chen, H.; Zhou, L.; Yuan, L.; Hoff, I. Characteristics and properties of asphalt mortar containing FO filler. *Constr. Build. Mater.* **2023**, *392*, 132039. [\[CrossRef\]](#)
42. Lou, B.; Sha, A.; Barbieri, D.M.; Liu, Z.; Zhang, F. Microwave heating properties of steel slag asphalt mixture using a coupled electromagnetic and heat transfer model. *Constr. Build. Mater.* **2021**, *291*, 123248. [\[CrossRef\]](#)
43. Zhu, H.; Yuan, H.; Liu, Y.; Fan, S.; Ding, Y. Evaluation of self-healing performance of asphalt concrete for macrocracks via microwave heating. *J. Mater. Civ. Eng.* **2020**, *32*, 04020248. [\[CrossRef\]](#)
44. Banerjee, A.; de Fortier Smit, A.; Prozzi, J.A. The effect of long-term aging on the rheology of warm mix asphalt binders. *Fuel* **2012**, *97*, 603–611. [\[CrossRef\]](#)
45. Bhasin, A.; Palvadi, S.; Little, D.N. Influence of aging and temperature on intrinsic healing of asphalt binders. *Transp. Res. Rec.* **2011**, *2207*, 70–78. [\[CrossRef\]](#)
46. Bera, A.; Babadagli, T. Status of electromagnetic heating for enhanced heavy oil/bitumen recovery and future prospects: A review. *Appl. Energy* **2015**, *151*, 206–226. [\[CrossRef\]](#)
47. Gao, J.; Sha, A.; Wang, Z.; Tong, Z.; Liu, Z. Utilization of steel slag as aggregate in asphalt mixtures for microwave deicing. *J. Clean. Prod.* **2017**, *152*, 429–442. [\[CrossRef\]](#)
48. Amani, S.; Kavussi, A.; Karimi, M.M. Effects of aging level on induced heating-healing properties of asphalt mixes. *Constr. Build. Mater.* **2020**, *263*, 120105. [\[CrossRef\]](#)
49. Poulikakos, L.D.; Hofko, B. A critical assessment of stiffness modulus and fatigue performance of plant produced asphalt concrete samples using various test methods. *Road Mater. Pavement Des.* **2021**, *22*, 2661–2673. [\[CrossRef\]](#)

Disclaimer/Publisher's Note: The statements, opinions and data contained in all publications are solely those of the individual author(s) and contributor(s) and not of MDPI and/or the editor(s). MDPI and/or the editor(s) disclaim responsibility for any injury to people or property resulting from any ideas, methods, instructions or products referred to in the content.